



Paper Type: Research Paper

FisPro Based Interpretable Fuzzy Inference System for Dual Circuit Extra High Voltage Transmission Line Fault Classification and Fault Distance Estimation

A Naresh Kumar^{1,*}  Sajja Suneel², Bharathi Gururaj³, Muktevi Chakravarthy⁴, Mortha Suresh Kumar⁵, Muniyappa Ramesha⁶, Elemasetty Uday Kiran⁷, Malleboina Nagaraju⁸

¹ Department of Electrical and Electronics Engineering, Institute of Aeronautical Engineering, Hyderabad, India; ankamnaresh29@gmail.com.

² Department of CSE (Data Science), Institute of Aeronautical Engineering, Hyderabad, India; sajja.suneel@gmail.com.

³ Department of Electronics and Communication Engineering, KS Institute of Technology, Bengaluru, India; a.nareshkumar@iare.ac.in.

⁴ Department of Electrical and Electronics Engineering, Vasavi College of Engineering, Hyderabad, India; chakri4330@gmail.com.

⁵ Department of Space Engineering, Ajeenka DY Patil University, Pune, India; morthasuresh@gmail.com.

⁶ Department of Electrical, Electronics and Communication Engineering, GITAM, Bengaluru, India; rameshmalur037@gmail.com.

⁷ Department of Aerospace Engineering, Toronto Metropolitan University, Toronto, Canada; eudaykiran95@gmail.com.

⁸ Department of Information Technology, University of the Cumberlands, Williamsburg, USA; nagaraju.fam50@gmail.com.

Citation:

Received: 17 April 2024

Revised: 14 July 2024

Accepted: 11 September 2024

Kumar, A. N., Suneel, S., Gururaj, B., Chakravarthy, M., Suresh Kumar, M. S., Ramesha, M., Kiran, E. U., & Nagaraju, M. (2025). FisPro based interpretable fuzzy inference system for dual circuit extra high voltage transmission line fault classification and fault distance estimation. *Journal of fuzzy extension and applications*, 6(3), 597-614.

Abstract

Accurate fault classification and precise fault distance estimation play a critical role in reliable, stable and optimal operation of electrical power systems. Especially Dual Circuit Extra High Voltage Transmission Line (DCEHVTI) fault diagnosis is a challenging task using conventional algorithms. Early fault recognition is crucial for DCEHVTI performance. Due to its effectiveness in classification and forecasting, the interpretable Mamdani Fuzzy Inference System (MFIS) is more suitable. Haar wavelet is efficient in any signal behavior evaluation. Therefore, this paper proposed a robust and intelligent Fuzzy Inference System Professional (FisPro) based interpretable MFIS with Haar wavelets transform for fault classification and fault distance estimation in DCEHVTI using single-side data. The dual circuit three-phase currents of two cycles are recorded from DCEHVTI. Haar wavelet transforms are utilized to estimate the behaviour and characteristics of the current signals in terms of high-frequency components. The captured fault currents from the DCEHVTI single side are used as inputs for the hierarchical MFIS framework. Here, the fault classification is followed by the faulty distance estimation in MFIS. The test results support the MFIS consistency under extensive changes in fault factors. Moreover, the extensive performance comparison study with the state of art fault diagnosis methods reiterates the FisPro based MFIS effectiveness in successful fault diagnosis. The obtained results indicate that MFIS has a fast processing time (in 1ms), high accuracy (above 99.8%), less fault location error (Within 0.0024%) and is useful for studying the system stability in the electricity field. The MFIS is proven to be successful for the fault diagnosis without any communication channel between the source and receiving end.

Keywords: Fuzzy inference system professional, Faults, Dual circuit, Accuracy.

1 | Introduction

Due to developments in society's living standards, the electricity demand is increasing every year. The power system is a network that employs numerous components to transfer electricity for performing different tasks.

 Corresponding Author: ankamnaresh29@gmail.com

 <https://doi.org/10.22105/jfea.2025.452949.1447>

 Licensee System Analytics. This article is an open access article distributed under the terms and conditions of the Creative Commons Attribution (CC BY) license (<http://creativecommons.org/licenses/by/4.0/>).

In the power system, transmission lines are essential links that achieve service continuity from the electricity generating stations to end customers. Nevertheless, transmission lines can experience different faults due to equipment failure, lightning strokes, heavy snowfall, high winds and insulation failure. Faults in transmission lines refer to any anomalous conditions that may occur in the transmission lines, disrupting the electricity flow. The faults in transmission lines can range from minor disruptions to severe disturbances, potentially leading to power outages, equipment damages, customer complaints, loss of revenue and even safety hazards. It must restore regular operation as quickly as possible and facilitate rapid response by the operators when faults occur in a transmission line. Detection, isolation and mitigation of transmission line faults promptly are necessary to reduce their impact on the power grid. Furthermore, the protective maintenance system helps to identify potential fault risks in transmission lines and address the faults before they lead to interruptions. Detection of faults and error calculations in electrical systems are addressed in [1–4]. The protective devices are manufactured to detect the faults remotely and isolate the transmission line affected part to prevent further damage.

The Extra High Voltage Transmission Lines (EHVTL) play a pivotal role in facilitating simple, efficient, stability and reliability. Its power transmission over long distances and energy security help to support economic developments and the transition to cleaner and extra sustainable energy resources. The EHVTL is constructed to carry electricity at higher voltages than traditional transmission lines. Faults are well studied in the literature, but only a few articles have explained EHVTL faults. Extensive research has been conducted to implement fault classification in EHVTL in the development of different effective techniques [5–7]. Recently, some good works for EHVTL fault classification have been reported [8], [9].

Several researchers have carried out protection schemes for EHVTL faults [10], [11]. The fault location approaches in EHVTL have been illustrated extensively in the past [12], [13]. Only a few researchers have studied the shunt faults in EHVTL using currents [14], [15]. Many methodologies are applied for fault location in EHVTL using remote terminal data [16], [17]. The neural networks method has been adopted for EHVTL fault location [18].

In the literature, various techniques have been illustrated for Dual Circuit Extra High Voltage Transmission Line (DCEHVT), but their protection using source end current has not been published up to date [19–22]. In [23], fault location analysis is done in DCEHVT using a neural network and support vector machine, but fault classification is ignored. Optimal control strategies for different systems are explained in [24], [25]. The research gaps and challenges in the previous research are as follows

- I. Support vector machines and neural networks need considerable training samples and time.
- II. Both end voltage and currents are used as input for the protection system.
- III. Performance metrics accuracy (%) is high and error (%) is low.
- IV. Difficult to design the protection model.
- V. The communication link between the source point and the receiving point is required.

1.1 | Novelty

The Mamdani Fuzzy Inference System (MFIS) algorithm is a popular adaptive and non-linear control system that gives robust performance during parameter uncertainties. The MFIS designing process is described in [26], [27]. The MFIS is frequently employed for the fault detection process. This system has the ability to consider the faults effectively in transmission lines. The application of MFIS to fault location in EHVTL has been reported in [28]. The MFIS fault location algorithm in transmission line focused which requires current measurements without considering far terminal information [29].

Naresh et al. [30] have explained fault classification, fault location and fault zone identification using MFIS [31], [32]. Some studies [33–35] using Fuzzy Inference System Professional (FisPro) based MFIS designing have been published. Fault location using MFIS has been presented in [36] for only dual circuit transmission

lines. The Haar-Cascade model for the detection problem is explained in [37]. Numerous fault diagnosis systems for dual circuit lines and EHVTL have been discussed separately using MFIS, but the field of MFIS-based fault diagnosis in DCEHVTL has not been developed yet. Hence, none of the previously published articles have provided a complete solution to protect DCEHVTL during shunt faults, considering single-end currents and MFIS. Thus, there is a need to design an effective protection technique that gives accurate fault detection in DCEHVTL without using remote terminal information. In this article, an efficient framework for classifying and locating faults in DCEHVTL using MFIS without considering far-end currents is proposed. Therefore, the contribution summary has mainly consisted of five aspects,

- I. Study of shunt fault behaviour.
- II. MFIS development using FisPro for fault classification and distance in DCEHVTL.
- III. Less computational burden.
- IV. Avoid the use of communication channels for source and receiving ends.
- V. Improvement of the accuracy, detection time and fault location error.

1.2 | Preliminaries

In this section, some helpful definitions related to fuzzy sets, Membership Functions (MSF), relation, and defuzzification are summarised.

Definition 1 ([38]). The fuzzy set M on a universal X is a set of ordered pairs:

$M = \{(x, \mu_M(x)) | x \in X\}$ where x is the generic element of X , $\mu_M: X \rightarrow [0, 1]$ is the MSF of fuzzy set M , $\mu_M(x) \in [0, 1]$ is the membership degree of the element x to fuzzy set M .

Definition 2. The curve that describes how each point in the input parameter is mapped to the membership value between 0 and 1 is called MSF [39].

Definition 3. A triangular MSF is specified by three parameters $\{k, l, m\}$ and can be expressed as follows [40]:

$$\text{Triangle } (x; k, l, m) = \begin{cases} 0, & x \leq k, \\ \frac{x-k}{l-k}, & k \leq x \leq l, \\ \frac{m-x}{m-l}, & l \leq x \leq m, \\ 0, & \text{otherwise.} \end{cases}$$

A triangular fuzzy number should be used if the MSF is known to be symmetrical and the maximum point is known. Three vertices state triangular fuzzy numbers: Left-end vertex, maximum vertex and right-end vertex.

Definition 4 ([41]). A trapezoidal MSF is specified by four parameters $\{k, l, m, n\}$ and can be formulated as follows:

$$\text{Trapezoidal } (x; k, l, m, n) = \begin{cases} 0, & x \leq k, \\ \frac{x-k}{l-k}, & k \leq x \leq l, \\ 1, & l \leq x \leq m, \\ \frac{n-x}{n-m}, & m \leq x \leq n, \\ 0, & \text{otherwise.} \end{cases}$$

A trapezoidal fuzzy number should be employed if the asymmetry of the MSF is known and the support values are known. Four vertices state trapezoidal fuzzy numbers: Left end vertex, left support vertex, right end vertex, and right support vertex.

Definition 5 ([39]). The cartesian product of two fuzzy sets is known as a fuzzy relation.

This paper is structured remaining sections as follows. The shunt faults in DCEHVTL and the feature extraction method are elucidated in Section 2. The MFIS designing in DCEHVTL for fault diagnosis is exemplified in Section 3. The experimental results and comparative study are illustrated in Section 4 and Section 5, respectively, and lastly, concluding remarks are extracted in Section 6.

2 | The Dual Circuit Extra High Voltage Transmission Line under Study

The DCEHVTL operates at significantly high voltages compared to low voltage transmission lines for minimisation of energy losses, whereas a large amount of electrical power transmission over longer distances. In this study, the implementation of the MFIS method using FisPro for fault diagnosis is focused. To test the proposed method performance-based classifier and locator, the line extending between both ends (Receiving and source) is considered. The length considered is 150 km having a source end voltage operates at 440 kV. It is designed in MATLAB, and a single line diagram is depicted in *Fig. 1*. Here, a large number of fault data are simulated with changes in different fault conditions in MATLAB.

The classification and distance calculation has been carried out with FisPro Software. This scheme requires only source end fault current data. The current transformer collects six currents of two circuits in DCEHVTL and pre-processed. The current transformers provide three-phase fault current magnitudes, enabling accurate and timely faulty diagnosis. During pre-processing, six currents were sampled at a sampling frequency of 1200 Hz. Further, they have been processed by a normal second-ordered low-pass butterworth filter with of 480 Hz cut-off frequency. *Fig. 2* discusses the proposed work flowchart. The information about DCEHVTL is demonstrated in *Table 1*.

Haar wavelets are wavelet types called after Alfred Haar mathematician from Hungarian. Haar wavelet is a mathematical tool with the ability to handle complex signals with changing frequencies. This wavelet has two parts: one is the father wavelet, and another is the mother wavelet. Here, the father wavelet is a scaling function, and the mother wavelet is a wavelet function. Haar wavelet decomposes data into approximation and detailed coefficients at various resolution levels for efficient representation. Haar wavelet applications are data compression, feature extraction and noise reduction.

Furthermore, its computation simplicity makes it more attractive for application in real-time, image processing and embedded systems. The currents are processed using Haar wavelets to extract various output parameters, viz. detailed coefficients at level-3, wavelets energy squared detailed coefficients, and particular phase restored energy faulty detection. Wavelets have been an ideal selection for studying non-stationary current transients owing to handling frequency and time localisation and then deeper vision into signal dynamics during faults. Then, the normalized current signals have been used as input to the implementation of MFIS. *Fig. 3* shows the Haar wavelets feature extraction process.

Table 1. DCEHVTL information.

S/N	Factors	Values
1	Number of phases in each circuit	3
2	Number of circuits	2
3	Earth resistivity	100 $\Omega\text{-m}$
4	Reactance to resistance ratio	10
5	Voltage	440 kV
6	Length	150 km
7	Frequency	50 Hz



Fig. 1. The Single line diagram of DCEHVTL.

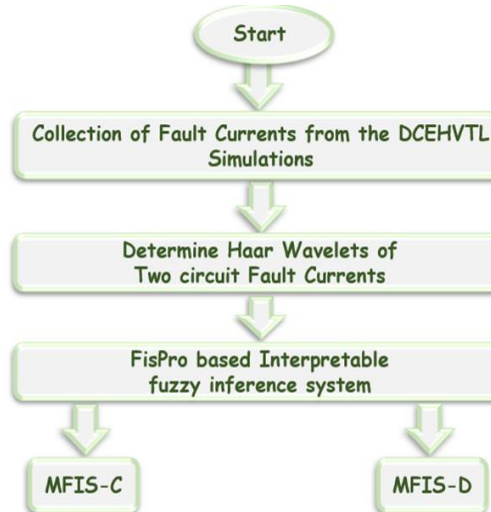


Fig. 2. The flow diagram of work.

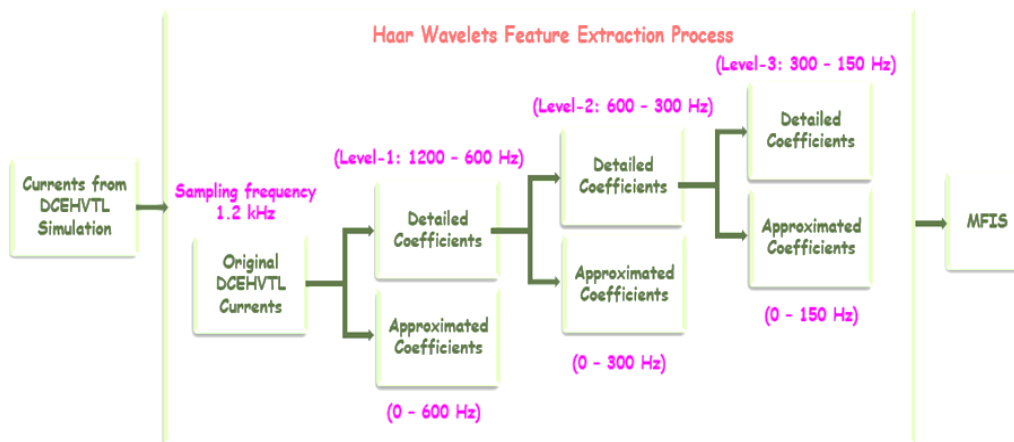


Fig. 3. Haar wavelets feature extraction.

3 | Fuzzy Inference System Professional-Based Mamdani Fuzzy Inference System

Fuzzy logic was entered into the scientific world by Zadeh [42] with the publication in 1965. It is a multi-valued logic in which variable truth values between 0 and 1. It can also be established in microcontrollers, natural language processing, control systems, image processing, software and hardware. Fuzzy logic can opt for a mathematical model that is employed in daily life applications and gives human behaviour understanding.

It is chosen in the computer to reflect human thoughts in classical logic inadequacy. The main task of a fuzzy system is the transfer of knowledge from human to computer. Rules store such knowledge. FisPro allows to development of fuzzy expert systems and to employ them for reasoning purposes, specifically for a biological or physical system simulation. Its establishment allows to make fuzzy systems from the rule expert knowledge base available in the particular field. It is flexible, robust, easy to implement, handles non-linear systems, mimics the human decision-making process and is more energy efficient. In short, an MFIS is a system that employs If-Then fuzzy rules defined by the domain-expert operator to make decisions about the output of the system behaviour. The FisPro-based MFIS can also used in classification and regression applications. Therefore, fault classification and fault distance of DCEHVTI can be estimated using FisPro-based MFIS.

Mamdani system is most commonly used in fuzzy applications due to its inherent characteristics of handling nonlinear relationships between inputs and outputs. Another type is the Sugeno system. It does not employ MSF and, it requires no defuzzification technique. The numerical output value is computed by rule weighted average consequent. MFIS was first introduced as a methodology to create a control scheme by synthesizing a linguistic control If-Then rule set collected from experienced human operators [43], [44]. The MFIS is an extended version classical rule system, which has If-Then rules composed of antecedents and consequents with fuzzy statements. The MFIS can be employed in numerous challenging sectors such as medicine, engineering, controlling and agriculture. The MFIS diagram is illustrated in *Fig. 4*. Here, the FisPro-based MFIS approaches the multi-input single output for fault location, i.e., MFIS-D and multi-input multi-output for classification, i.e., MFIS-C. The MFIS has a total of three main components: Fuzzy section, rule base section and defuzzification section.

3.1 | Fuzzification

The fuzzification transforms input crisp values into fuzzy sets. MSF is a graph that illustrates how each point in input space is assigned a value from 0 to 1 range. It employs MSF to associate a grade to each fuzzy set linguistic term. It adjusts the membership degree in fuzzy systems.

3.2 | Rulebase

The rule base connects inputs, which can be written rules as If-Then, to outputs. The If-Then is employed to find the input-output relationship values. The MSF converts precise input into linguistic variables in the fuzzification procedure. The inputs are used as fuzzy variables for the proposed MFIS. The max-min operation is most commonly employed. Fuzzy implication $M \rightarrow N$ as fuzzy relation. If "X is M," then "Y is N".

$$R = (M \times N) \cup (\bar{M} \times Y),$$

where μ_M and μ_N are two MSF of fuzzy sets M and N, respectively, and Y is the universe of discourse, same as N, but MSF is 1 for all. The MSF of R is chosen by

$$\mu_R(x,y) = \max \left(\min(\mu_M(x), \mu_N(y)), 1 - \mu_M(x) \right).$$

3.3 | Defuzzification

Lastly, the fuzzy values generated by the rulebase system are transformed into a numerical value by the defuzzification technique. In this, the linguistic variable accepts a correct crisp value. The most commonly used method is the centroid area technique. It is also known as the centre of gravity technique; the MFIS first computes the area under the scaled MSF and within the output variable range. It effectively determines the best compromise between the multiple output linguistic variables. The following equation calculates the geometric centre of the area:

$$x^* = \frac{\int \mu_c(x) \cdot x dx}{\int \mu_c(x) dx},$$

where x -linguistic variable value and x^* -centre of area.

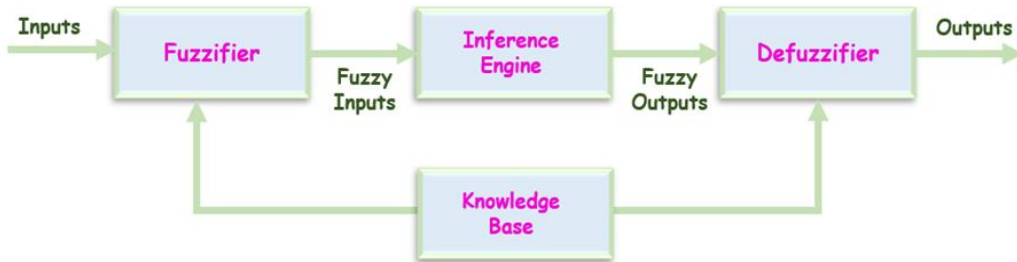


Fig. 4. The MFIS diagram.

Numerous software tools are proposed to create and design MFIS. Mamdani type of fuzzy system using FisPro software is employed in this work. Two MFIS acting as fault classifier (MFIS-C) and fault distance locator (MFIS-D) are made by FisPro, demonstrated in *Table 2*. The MFIS-C is based on the multiple input and multiple output Mamdani model of fuzzy type. Here, the number of inputs and outputs of MFIS-C are 6 (Fault currents) and 6 (Fault phases), respectively, as shown in *Fig. 5*. There are inputs for MFIS-C, which include currents so that output changes in phases. Each input is labelled as S_{Ia1}, S_{Ib1}, S_{Ic1}, S_{Ia2}, S_{Ib2} and S_{Ic2}. The trapezoidal MSF is a piecewise linear and trapezoidal, which can provide vague information data caused by linguistic calculations by converting them into crisp variables objectively. Each input of MFIS-C is fuzzified into 2 parts with the help of trapezoidal MSF denoted Low_Current and High_Current, as depicted in *Fig. 6*. Each output is labelled as FA₁, FB₁, FC₁, FA₂, FB₂ and FC₂. The triangular MSF is typically used due to its simplicity and good computational efficiency. Each output to MFIS-C is assigned the triangular MSF denoted H and F, as depicted in *Fig. 7*. When the fault occurs, the current magnitudes increase to high in faulty phases, whereas the current magnitudes do not vary in the healthy phases. When the current magnitude changes from healthy are recognised, then faults can be detected from the MFIS-C. After the fuzzification procedure is done, the next step is to make the If-Then rules. *Fig. 8* lists If-Then rules expressed in MFIS-C according to changes in healthy and fault currents for fault classification. The number of IF-Then rules is attained by multiplying with number of inputs by each other, which is equivalent to 64. The AND operator joins the antecedent and consequent fuzzy MSF in each rule according to the relation between input and output.

Where, S_{Ia1}: source current in phase-A of circuit-1.

S_{Ib1}: Source current in phase-B of circuit-1.

S_{Ic1}: Source current in phase-C of circuit-1.

S_{Ia2}: Source current in phase-A of circuit-2.

S_{Ib2}: Source current in phase-B of circuit-2.

S_{Ic2}: Source current in phase-C of circuit-2.

FA₁: Faulty phase-A of circuit-1.

FB₁: Faulty phase-B of circuit-1.

FC₁: Faulty Phase-C of circuit-1.

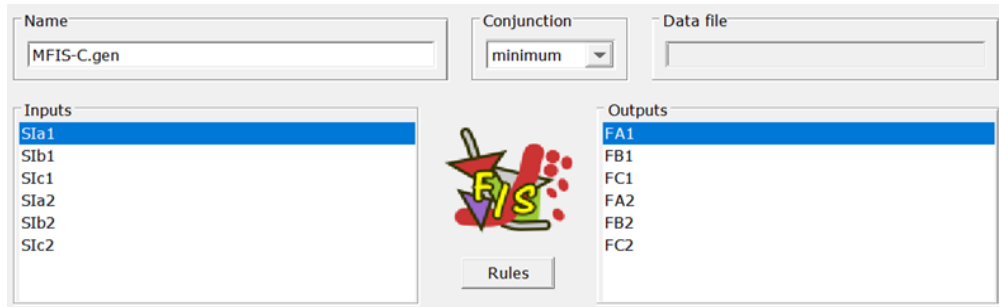
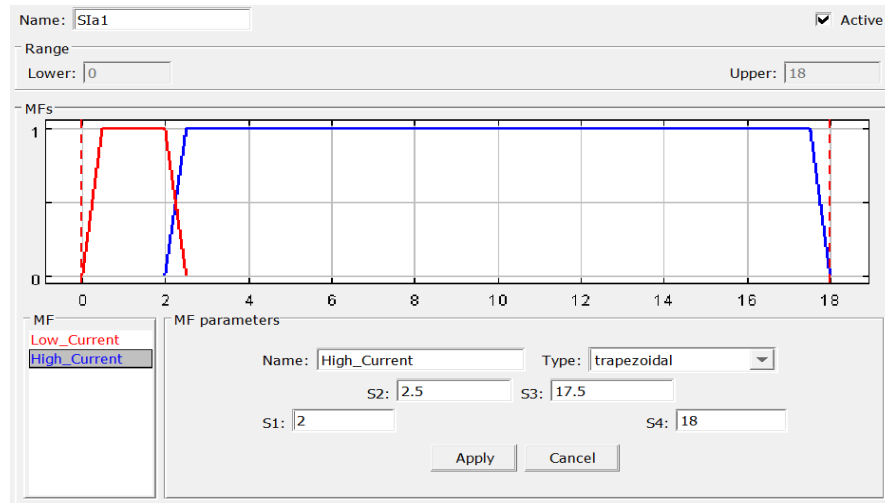
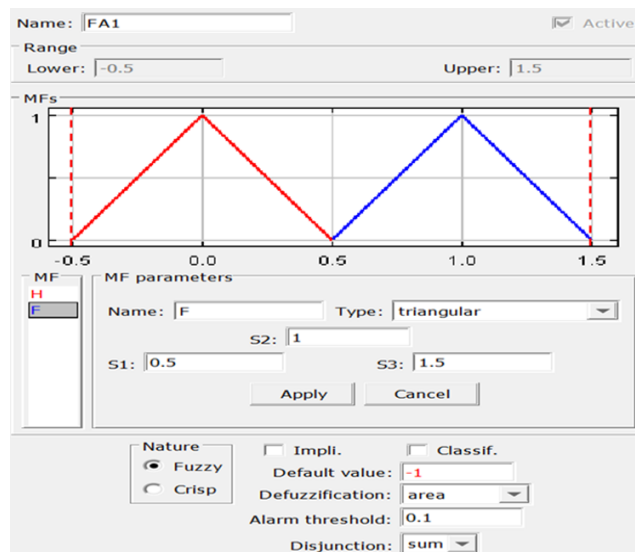
FA₂: Faulty phase-A of circuit-2.

FB₂: Faulty phase-B of circuit-2.

FC₂: Faulty phase-C of circuit-2.

Table 2. MFIS structures.

System	Inputs	Linguistic Variables	Type of MSF	MSF Names
MFES-C	Inputs (6)	SIa1, SIb1, SIC1, SIa2, SIb2, SIC2	Trapezoidal	Low-current, high-current
	Outputs (6)	FA1, FB1, FC1, FA2, FB2, FC2	Triangular	H, F
MFES-D	Inputs (6)	SIa1, SIb1, SIC1, SIa2, SIb2, SIC2	Triangular	I-H, I-I, I-J
	Output (1)	Distance	Triangular	H, I, J

**Fig. 5. Input and output of MFIS-C.****Fig. 6. MSF of each input for MFIS-C.****Fig. 7. MSF of each output for MFIS-C.**

Rule	Active	IF S1a1	AND S1b1	AND S1c1	AND S1a2	AND S1b2	AND S1c2	THEN FA1	FB1	FC1	FA2	FB2	FC2
1	✓	Low_Current	Low_Current	Low_Current	Low_Current	Low_Current	Low_Current	H	H	H	H	H	H
2	✓	Low_Current	Low_Current	Low_Current	Low_Current	Low_Current	High_Current	H	H	H	H	H	F
3	✓	Low_Current	Low_Current	Low_Current	Low_Current	High_Current	Low_Current	H	H	H	H	F	H
4	✓	Low_Current	Low_Current	Low_Current	Low_Current	High_Current	High_Current	H	H	H	H	F	F
5	✓	Low_Current	Low_Current	Low_Current	High_Current	Low_Current	Low_Current	H	H	H	F	H	H
6	✓	Low_Current	Low_Current	Low_Current	High_Current	Low_Current	High_Current	H	H	H	F	H	F
7	✓	Low_Current	Low_Current	Low_Current	High_Current	High_Current	Low_Current	H	H	H	F	F	H
8	✓	Low_Current	Low_Current	Low_Current	High_Current	High_Current	High_Current	H	H	H	F	F	F
9	✓	Low_Current	Low_Current	High_Current	Low_Current	Low_Current	Low_Current	H	H	F	H	H	H
10	✓	Low_Current	Low_Current	High_Current	Low_Current	Low_Current	High_Current	H	H	F	H	H	F
11	✓	Low_Current	Low_Current	High_Current	Low_Current	High_Current	Low_Current	H	H	F	H	F	H
12	✓	Low_Current	Low_Current	High_Current	Low_Current	High_Current	High_Current	H	H	F	H	F	F
13	✓	Low_Current	Low_Current	High_Current	High_Current	Low_Current	Low_Current	H	H	F	F	H	H
14	✓	Low_Current	Low_Current	High_Current	High_Current	Low_Current	High_Current	H	H	F	F	H	F
15	✓	Low_Current	Low_Current	High_Current	High_Current	High_Current	Low_Current	H	H	F	F	F	H
16	✓	Low_Current	Low_Current	High_Current	High_Current	High_Current	High_Current	H	H	F	F	F	F
17	✓	Low_Current	High_Current	Low_Current	Low_Current	Low_Current	Low_Current	H	F	H	H	H	H
18	✓	Low_Current	High_Current	Low_Current	Low_Current	Low_Current	High_Current	H	F	H	H	H	F
19	✓	Low_Current	High_Current	Low_Current	Low_Current	High_Current	Low_Current	H	F	H	H	F	H
20	✓	Low_Current	High_Current	Low_Current	Low_Current	High_Current	High_Current	H	F	H	H	F	F
21	✓	Low_Current	High_Current	Low_Current	High_Current	Low_Current	Low_Current	H	F	H	F	H	H
22	✓	Low_Current	High_Current	Low_Current	High_Current	Low_Current	High_Current	H	F	H	F	H	F
23	✓	Low_Current	High_Current	Low_Current	High_Current	High_Current	Low_Current	H	F	H	F	F	H
24	✓	Low_Current	High_Current	Low_Current	High_Current	High_Current	High_Current	H	F	H	F	F	F
25	✓	Low_Current	High_Current	High_Current	Low_Current	Low_Current	Low_Current	H	F	F	H	H	H
26	✓	Low_Current	High_Current	High_Current	Low_Current	Low_Current	High_Current	H	F	F	H	H	F
27	✓	Low_Current	High_Current	High_Current	Low_Current	Low_Current	High_Current	H	F	F	H	F	H
28	✓	Low_Current	High_Current	High_Current	Low_Current	High_Current	Low_Current	H	F	F	H	F	F
29	✓	Low_Current	High_Current	High_Current	High_Current	Low_Current	Low_Current	H	F	F	F	H	H
30	✓	Low_Current	High_Current	High_Current	High_Current	Low_Current	High_Current	H	F	F	F	H	F
31	✓	Low_Current	High_Current	High_Current	High_Current	High_Current	Low_Current	H	F	F	F	F	H
32	✓	Low_Current	High_Current	High_Current	High_Current	High_Current	High_Current	H	F	F	F	F	F
33	✓	High_Current	Low_Current	Low_Current	Low_Current	Low_Current	Low_Current	F	H	H	H	H	H
34	✓	High_Current	Low_Current	Low_Current	Low_Current	Low_Current	High_Current	F	H	H	H	H	F
35	✓	High_Current	Low_Current	Low_Current	Low_Current	High_Current	Low_Current	F	H	H	H	F	H
36	✓	High_Current	Low_Current	Low_Current	Low_Current	High_Current	High_Current	F	H	H	H	F	F
37	✓	High_Current	Low_Current	Low_Current	High_Current	Low_Current	Low_Current	F	H	H	F	H	H
38	✓	High_Current	Low_Current	Low_Current	High_Current	Low_Current	High_Current	F	H	H	F	H	F
39	✓	High_Current	Low_Current	Low_Current	High_Current	High_Current	Low_Current	F	H	H	F	F	H
40	✓	High_Current	Low_Current	Low_Current	High_Current	High_Current	High_Current	F	H	H	F	F	F
41	✓	High_Current	Low_Current	High_Current	Low_Current	Low_Current	Low_Current	F	H	F	H	H	H
42	✓	High_Current	Low_Current	High_Current	Low_Current	Low_Current	High_Current	F	H	F	H	H	F
43	✓	High_Current	Low_Current	High_Current	Low_Current	High_Current	Low_Current	F	H	F	H	F	H
44	✓	High_Current	Low_Current	High_Current	Low_Current	High_Current	High_Current	F	H	F	H	F	F
45	✓	High_Current	Low_Current	High_Current	High_Current	Low_Current	Low_Current	F	H	F	F	H	H
46	✓	High_Current	Low_Current	High_Current	High_Current	Low_Current	High_Current	F	H	F	F	H	F
47	✓	High_Current	Low_Current	High_Current	High_Current	High_Current	Low_Current	F	H	F	F	F	H
48	✓	High_Current	Low_Current	High_Current	High_Current	High_Current	High_Current	F	H	F	F	F	F
49	✓	High_Current	High_Current	Low_Current	Low_Current	Low_Current	Low_Current	F	F	H	H	H	H
50	✓	High_Current	High_Current	Low_Current	Low_Current	Low_Current	High_Current	F	F	H	H	H	F
51	✓	High_Current	High_Current	Low_Current	Low_Current	High_Current	Low_Current	F	F	H	H	F	H
52	✓	High_Current	High_Current	Low_Current	Low_Current	Low_Current	High_Current	F	F	H	H	F	F
53	✓	High_Current	High_Current	Low_Current	High_Current	Low_Current	Low_Current	F	F	H	F	H	H
54	✓	High_Current	High_Current	Low_Current	High_Current	Low_Current	High_Current	F	F	H	F	H	F
55	✓	High_Current	High_Current	Low_Current	High_Current	High_Current	Low_Current	F	F	H	F	F	H
56	✓	High_Current	High_Current	Low_Current	High_Current	High_Current	High_Current	F	F	H	F	F	F
57	✓	High_Current	High_Current	High_Current	Low_Current	Low_Current	Low_Current	F	F	F	H	H	H
58	✓	High_Current	High_Current	High_Current	Low_Current	Low_Current	High_Current	F	F	F	H	H	F
59	✓	High_Current	High_Current	High_Current	Low_Current	High_Current	Low_Current	F	F	F	H	F	H
60	✓	High_Current	High_Current	High_Current	Low_Current	High_Current	High_Current	F	F	F	H	F	F
61	✓	High_Current	High_Current	High_Current	High_Current	Low_Current	Low_Current	F	F	F	F	H	H
62	✓	High_Current	High_Current	High_Current	High_Current	High_Current	Low_Current	F	F	F	F	H	F
63	✓	High_Current	High_Current	High_Current	High_Current	High_Current	High_Current	F	F	F	F	F	H
64	✓	High_Current	High_Current	High_Current	High_Current	High_Current	High_Current	F	F	F	F	F	F

Fig. 8. MFIS-C If-Then rules.

Similarly, MFIS-D is based on the multiple input and single output Mamdani model of fuzzy type. The number of inputs and outputs of MFIS-D are 6 (Fault currents) and 1 (Fault location), respectively, as explained in Fig. 9. There are inputs for MFIS-D, which include currents so that output changes in fault distance. Each input is labelled as S1a1, S1b1, S1c1, S1a2, S1b2 and S1c2. Each input is fuzzified into 3 parts with the help of triangular MSF denoted I-H, I-I and I-J, as depicted in Fig. 10. The output is labelled as distance. The output to MFIS-D is assigned the triangular MSF denoted H, I and J, as depicted in Fig. 11. The number of IF-Then rules is attained by multiplying with number of inputs by each other, which is equivalent to 42. Due to its superiority in the particular equivalence relation, the max-min operation is adopted for fuzzy inference, and the centroid area technique is used in the defuzzification procedure. In the If-Then rules, logical operation, implication and aggregation operations are carried out. The antecedents use the logic “AND”, implication uses the function “min,” and aggregation uses the function “max” of the Mamdani system. The fault current magnitude decreases from the source end to the receiving end. Thus, fault current increase's

fault location from the source decreases. Fault distance is inversely proportional to fault current. Therefore, MFIS-D output fault location is based on the fault current magnitudes. Fig. 12 lists If-Then rules expressed in MFIS-D. It determines fault location with a given output range (1-150) based on If-Then rules according to the relation fault location and fault current from the source. Now, the MFIS-C and MFIS-D receive all inputs as an output of phases and location, respectively.

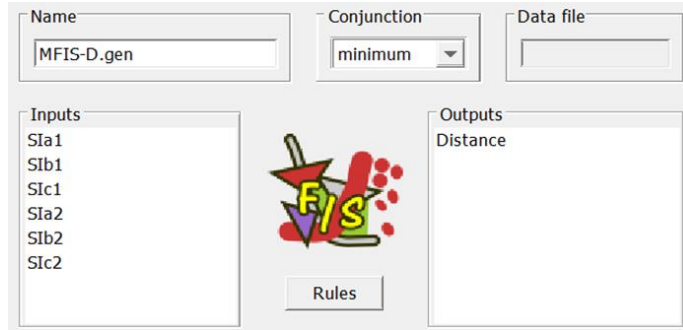


Fig. 9. Input and output of MFIS-D.

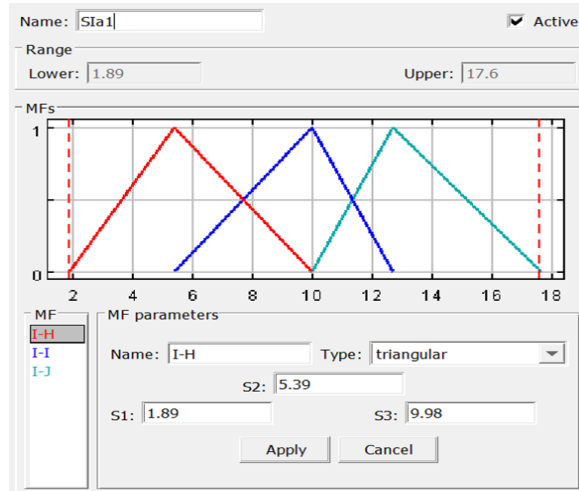


Fig. 10. MSF of each input for MFIS-D.

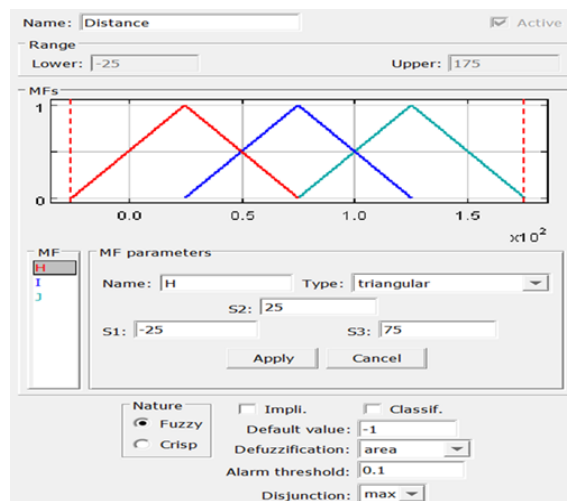


Fig. 11. MSF of each output for MFIS-D.

Rule	Active	IF Sla1	AND Sib1	AND Sic1	AND Sla2	AND Sib2	AND Sic2	THEN Di...
1	✓					I-H		J
2	✓					I-I		I
3	✓					I-J		H
4	✓				I-H			J
5	✓				I-I			I
6	✓				I-J			H
7	✓			I-H				J
8	✓			I-I				I
9	✓			I-J				H
10	✓				I-H	I-H		J
11	✓				I-I	I-I		I
12	✓				I-J	I-J		H
13	✓			I-H		I-H		J
14	✓			I-I		I-I		I
15	✓			I-J		I-J		H
16	✓				I-H	I-H		J
17	✓				I-I	I-I		I
18	✓				I-J	I-J		H
19	✓			I-H	I-H	I-H		J
20	✓			I-I	I-I	I-I		I
21	✓			I-J	I-J	I-J		H
22	✓		I-H					H
23	✓		I-I					J
24	✓		I-J					I
25	✓	I-H						H
26	✓	I-I						J
27	✓	I-J						I
28	✓	I-H						H
29	✓	I-I						J
30	✓	I-J						I
31	✓		I-H	I-H				H
32	✓		I-I	I-I				J
33	✓		I-J	I-J				I
34	✓	I-H		I-H				H
35	✓	I-I		I-I				J
36	✓	I-J		I-J				I
37	✓		I-H	I-H				H
38	✓		I-I	I-I				J
39	✓		I-J	I-J				I
40	✓	I-H	I-H	I-H				H
41	✓	I-I	I-I	I-I				J
42	✓	I-J	I-J	I-J				I

Fig. 12. MFIS-D If-Then rules.

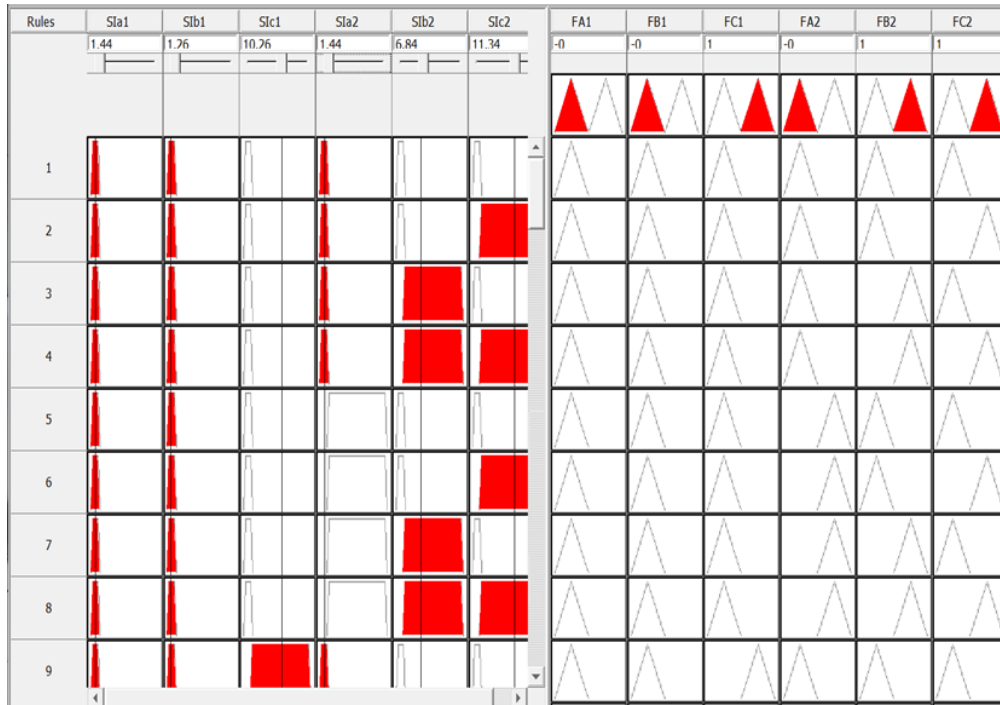
4 | Results

In this study, the performance of FisPro-based MFIS has been checked for DCEHVTL fault classification and location under numerous fault factors such as fault type, fault location, fault switching time and fault resistance. A total of 14000 cases are employed for investigating MFIS-based algorithm performance. The reliability of MFIS-C and MFIS-D have been assessed based on statistical metrics such as accuracy (%) and error (%). Here, high accuracy (%) shows the quality of phase identification in the fault and low error (%) illustrates the exactness of fault distance estimation. The accuracy (%) and error (%) equations derivation are explained in [27]. The results of this study are revealed in the next subsections.

$$\text{Accuracy (\%)} = \frac{\text{Correctly classified samples}}{\text{Total samples}}. \quad (1)$$

$$\text{Error (\%)} = \left| \frac{\text{DA (km)} - \text{DE (km)}}{\text{Length}} \right| \times 100. \quad (2)$$

The performance of MFIS-C has been explored for numerous fault scenarios, and simulations have been done on DCEHVTL in MATLAB software. *Table 3* reports the MFIS-C results in DCEHVTL. The *Eq. (1)* exemplifies MFIS-C output accuracy calculation. An effective fault classification scheme is essential for maintaining safety, reliability and DCEHVTL performance. The output of the MFIS-C value is either 1 or 0 based on the faulty and healthy cases. The MFIS-C accuracy lies between 99.98% and 99.99%, as listed in *Table 3*. The classifier behaviour also validates the obtained results correctly during the offline study. It is confirmed that fault scenarios do not affect the MFIS-C performance for most of the test samples. One sample result for the B2C2 fault at 21 km is depicted in *Fig. 13*. It is clear that the detection time is within one post-fault cycle time.

**Fig. 13. MFIS-C one sample output.**

The performance of MFIS-D has been assessed for different fault samples, and simulations have been done on DCEHVT in MATLAB software. *Table 3* reports the MFIS-D results in DCEHVT. The *Eq. (2)* illustrates MFIS-D output error calculation. The fault location is crucial for diagnosing and resolving problems effectively, especially in complex transmission systems where the faults can have diverse causes and manifestations. The output of MFIS-D value is between 0 to 150 based on current magnitudes. The MFIS-D error lies between 0.0002% and 0.0024%, as listed in *Table 3*. The fault locator behaviour confirms the attained simulation results effectively during the offline study. It is noted that fault cases do not influence the MFIS-D performance for numerous tests. One sample result for the B2C2 fault at 37 km is shown in *Fig. 14*. It is evident that response time is very fast processing time. The best performance metrics (accuracy (%) and error (%)) by changing different fault parameters from the test results are addressed in *Fig. 15*.

Table 3. Test results for MFIS-C and MFIS-D.

Parameter	Fault Type	I($^{\circ}$)	R(Ω)	MFIS-D			MFIS-C					
				D _A (Km)	D _E (Km)	Error (%)	A1	B1	C1	A2	B2	C2
Changing faults and constant D(km), I ($^{\circ}$), R(Ω)	A1B1	190	32	121	121.351	0.0023	1	1	0	0	0	0
	A1C1	190	32	121	120.824	0.0011	1	0	1	0	0	0
	B1C1	190	32	121	121.252	0.0016	0	1	1	0	0	0
	A2B2	190	32	121	121.086	0.0005	1	1	1	0	0	0
	A2C2	190	32	121	120.793	0.0013	0	0	0	1	1	0
	B2C2	190	32	121	121.219	0.0014	0	0	0	1	0	1
	A1B1C1	190	32	121	121.147	0.0009	0	0	0	0	1	1
	A2B2C2	190	32	121	121.316	0.0021	0	0	0	1	1	1
Changing D(km) and constant faults, I ($^{\circ}$), R(Ω)	A2C2	125	63	06	06.208	0.0013	0	0	0	1	0	1
	A2C2	125	63	26	26.363	0.0024	0	0	0	1	0	1
	A2C2	125	63	46	45.849	0.0010	0	0	0	1	0	1
	A2C2	125	63	66	65.915	0.0005	0	0	0	1	0	1
	A2C2	125	63	86	86.152	0.0010	0	0	0	1	0	1
	A2C2	125	63	106	106.275	0.0018	0	0	0	1	0	1
	A2C2	125	63	126	126.094	0.0006	0	0	0	1	0	1
	A2C2	125	63	146	146.310	0.0020	0	0	0	1	0	1

Table 3. Continued.

Parameter	Fault Type	I($^{\circ}$)	R(Ω)	MFIS-D			MFIS-C					
				D _A (Km)	D _A (Km)	D _A (Km)	A1	B1	C1	A2	B2	C2
Changing I($^{\circ}$) and constant faults, D(km), R(Ω)	A1B1	10	18	59	58.926	0.0004	1	1	0	0	0	0
	A1B1	60	18	59	59.362	0.0024	1	1	0	0	0	0
	A1B1	110	18	59	59.329	0.0021	1	1	0	0	0	0
	A1B1	160	18	59	59.183	0.0012	1	1	0	0	0	0
	A1B1	210	18	59	59.286	0.0019	1	1	0	0	0	0
	A1B1	260	18	59	58.881	0.0007	1	1	0	0	0	0
	A1B1	310	18	59	59.158	0.0010	1	1	0	0	0	0
	A1B1	360	18	59	59.032	0.0002	1	1	0	0	0	0
Changing R(Ω) and constant faults, D(km), I($^{\circ}$)	A2B2C2	35	4	143	143.285	0.0018	0	0	0	1	1	1
	A2B2C2	35	14	143	143.139	0.0009	0	0	0	1	1	1
	A2B2C2	35	24	143	142.746	0.0016	0	0	0	1	1	1
	A2B2C2	35	34	143	143.109	0.0007	0	0	0	1	1	1
	A2B2C2	35	44	143	143.357	0.0023	0	0	0	1	1	1
	A2B2C2	35	54	143	143.342	0.0022	0	0	0	1	1	1
	A2B2C2	35	64	143	142.802	0.0013	0	0	0	1	1	1
	A2B2C2	35	74	143	143.229	0.0015	0	0	0	1	1	1

Where DA-actual fault location/distance.

DE: Estimation fault location/distance.

A1: Phase A in circuit 1 of DCEHVTL.

B1: Phase B in circuit 1 of DCEHVTL.

C1: Phase C in circuit 1 of DCEHVTL.

A2: Phase A in circuit 2 of DCEHVTL.

B2: Phase B in circuit 2 of DCEHVTL.

C2: Phase C in circuit 2 of DCEHVTL.

R: Resistance.

I: Switching time.

D: Distance.

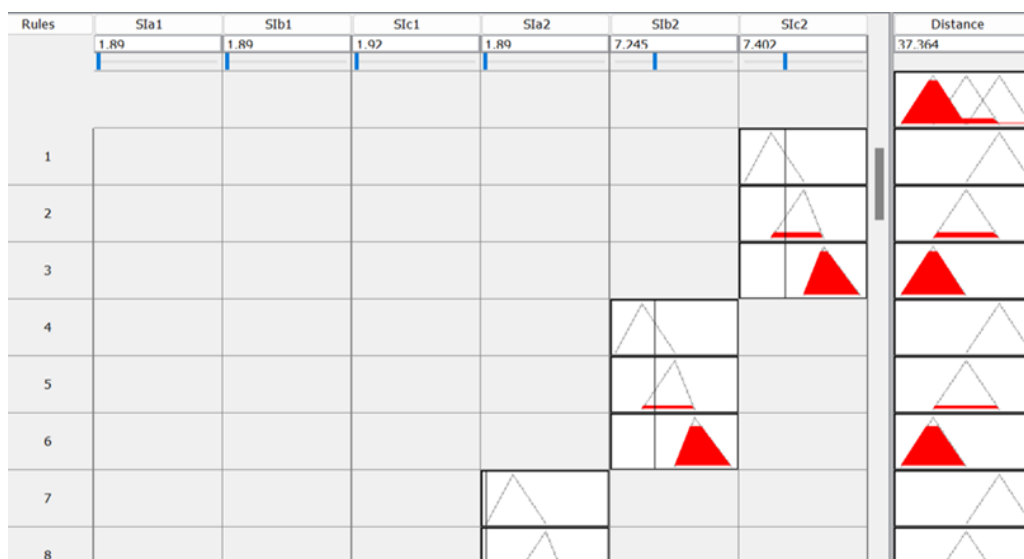


Fig. 14. MFIS-D one sample output.

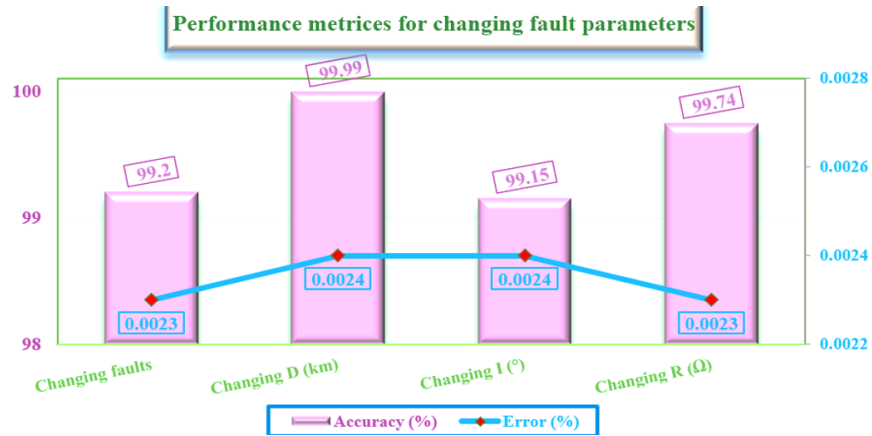


Fig. 15. The performance metrices for changing fault parameters.

5 | Analysing the Present Technique with Existing Methods

The findings of the proposed study in DCEHVTL for classifying and locating faults are compared with other existing methods in *Table 4*. In [15], [29] fault classification and location in line using neural network. The disadvantage of the neural network-based technique is that it needs sample training, which requires a large number of samples, hidden layers, neurons, transfer function, training method and epochs. The response time MFIS is below half a cycle from inception of fault, which is compared to methods in [15], [29], [32]. As compared to [39], MFIS achieves similar accuracy and better fault distance error. Therefore, MFIS is a better selection of DCEHVTL fault classification and fault location.

Table 4. Comparison study.

Article	Inputs Used	Fault Protection Function	Method	Time	Accuracy (%)	Error (%)
[15]	Sending end instantaneous currents and voltages	Classification and distance calculation	Neural networks	One cycle	-	0.3041
[17]	Source end currents and voltages	Distance calculation	Radial basis function neural networks	-	-	0.5
[23]	One end positive sequence currents and voltages	Distance calculation	Neural networks	0.0002 Sec	-	0.0787
[29]	Relay end currents and voltages	Classification and distance calculation	MFIS	Half cycle	99	5
[32]	Sending end impedances, currents and voltages	Classification and distance calculation	MFIS	One cycle	-	0.504
[36]	Sending end currents only	Classification and distance calculation	MFIS	-	99.98	0.3200
Proposed	Source end currents	Classification and distance calculation	MFIS	Half cycle	99.99	0.0024

6 | Conclusion

The ability to diagnose faults in overhead lines is of prime importance for the economic operation of the power system. An effective fault classification and distance estimation in DCEHVTL based on MFIS was focused on in this study. To deal with this issue, various preprocessing stages, which include mainly feature selection, feature extraction and dimension reduction for faulty classification and distance estimation, have been proposed. The most common methods used in the preprocessing stage are Haar wavelets. The three-phase wavelet fault currents of DCEHVTL are used as inputs to MFIS. The core parts of MFIS are fuzzifier, rule inference and defuzzifier. The comparison study of neural networks, FisPro-based MFIS support vector machine shows that FisPro software MFIS gives more accuracy in classifying and locating faults. The obtained results of FisPro software-based MFIS have been shown under different fault scenarios. The attained results note that the proposed MFIS based on FisPro is capable of classifying and locating faults with better accuracy and less error. Various sensitivity studies have been conducted for the effect of parameter changing (Fault type, fault location, fault switching time and fault resistance) on MFIS output. Fault accuracy of above 99.8 % and fault location error of a maximum of 0.0024% is obtained when identifying all faults. Therefore, the FisPro protection scheme can be employed for fault type identification and distance estimation in DCEHVTL. Nonetheless, research work was not validated for zone protection and other machine-learning techniques. This work can develop fault classification and location methods using a support vector machine, k-nearest neighbour algorithm, and artificial neural networks method and compare results with MFIS. It can also develop an MFIS for complete zone protection of DCEHVTL against the faults.

Acknowledgments

The authors are indebted to the reviewers for their very careful reading and valuable comments.

Author Contribution

Conceptualization, A.N., and M.C.; Methodology, A.N., S.S., and B.G.; Software, S.S., M.C., and B.G.; Validation, A.N., M.R., and B.G.; formal analysis, M.C., B.G., and M.S.; investigation, A.N., S.S., and M.R.; resources, M.R.; data maintenance, M.R., M.S. and B.G.; writing-creating the initial design, A.N., and E.U.; writing-reviewing and editing, A.N., E.U., and M.N.; visualization, E.U., and M.S.; monitoring, S.S., M.C., and M.N.; project management, S.S., M.S., and M.N. All authors have read and agreed to the published version of the manuscript.

Funding

No funding

Data Availability

The data is provided in the manuscript.

Conflicts of Interest

The authors declare that they have no competing interests.

References

- [1] Meslami, W., & Kamoun, T. (2021). Detection of an imbalance fault by vibration monitoring: Case of a screw compressor. *Journal of applied research on industrial engineering*, 8(1), 27–39.
<https://doi.org/10.22105/jarie.2021.269384.1243>

[2] Metwaly, A. A., & Elhenawy, I. (2023). Sustainable intrusion detection in vehicular controller area networks using machine intelligence paradigm. *Sustainable machine intelligence journal*, 4, 1–4. <https://doi.org/10.61185/SMIJ.2023.44104>

[3] Saberi, M., & Taghipoor, B. (2018). Detect and categorize errors in smart grids using voltage and current phases. *Journal of decisions and operations research*, 3(1), 82–98. (In Persian). <https://doi.org/10.22105/dmor.2018.58265>

[4] Afzali Behbahani, N. (2021). Identification, evaluation and prioritization of hazards caused by high voltage power towers in urban areas. *Big data and computing visions*, 1(1), 7–14. <https://doi.org/10.22105/bdcv.2021.142091>

[5] He, Z., Fu, L., Lin, S., & Bo, Z. (2010). Fault detection and classification in EHV transmission line based on wavelet singular entropy. *IEEE transactions on power delivery*, 25(4), 2156–2163. <https://doi.org/10.1109/TPWRD.2010.2042624>

[6] Song, Y. H., Johns, A. T., Xuan, Q. Y., & Liu, J. Y. (1997). Genetic algorithm based neural networks applied to fault classification for ehv transmission lines with a upfc. *6th international conference on developments in power systems protection* (pp. 278–281). IET. <https://doi.org/10.1049/cp:19970081>

[7] Bouthiba, T. (2005). Fault detection and classification technique in EHV transmission lines based on artificial neural networks. *European transactions on electrical power*, 15(5), 443–454. <https://doi.org/10.1002/etep.58>

[8] Raval, P. D., & Pandya, A. S. (2022). A hybrid PSO-ANN-based fault classification system for EHV transmission lines. *IETE journal of research*, 68(4), 3086–3099. <https://doi.org/10.1080/03772063.2020.1754299>

[9] Raval, P. D., & Pandya, A. S. (2016). Improved fault classification in series compensated ehv transmission line using wavelet transform and artificial neural network. *2016 IEEE 1st international conference on power electronics, intelligent control and energy systems (ICPEICES)* (pp. 1–5). IEEE. <https://doi.org/10.1109/ICPEICES.2016.7853543>

[10] Shu, H., Tian, K., Tang, Y., & Dai, Y. (2024). Novel protection scheme for EHV transmission line based on traveling wave energy. *Electric power systems research*, 230, 110247. <https://doi.org/10.1016/j.epsr.2024.110247>

[11] Zhen-tao, I., Iang-gen, I., Zhe, Z., Jing-chao, A., & Ong-jun, I. (2004). Studies of ehv transmission lines protection based on power balance. *39th international universities power engineering conference, 2004. UPEC 2004* (Vol. 2, pp. 742–746). IEEE. <https://ieeexplore.ieee.org/abstract/document/1492119>

[12] Gergis, A. A., Hart, D. G., & Peterson, W. L. (2002). A new fault location technique for two-and three-terminal lines. *IEEE transactions on power delivery*, 7(1), 98–107. <https://doi.org/10.1109/61.108895>

[13] Li, H., Gan, Y., Liu, H., Zheng, Z., Zhang, Y., & Zhang, F. (2015). Advanced fault location system for ehv transmission lines. *2015 5th international conference on electric utility deregulation and restructuring and power technologies (DRPT)* (pp. 999–1003). IEEE. <https://doi.org/10.1109/DRPT.2015.7432376>

[14] Chen, J., & Aggarwal, R. K. (2012). A new approach to ehv transmission line fault classification and fault detection based on the wavelet transform and artificial intelligence. *2012 IEEE power and energy society general meeting* (pp. 1–8). IEEE. <https://doi.org/10.1109/PESGM.2012.6344762>

[15] Ben Hessine, M., & Ben Saber, S. (2014). Accurate fault classifier and locator for EHV transmission lines based on artificial neural networks. *Mathematical problems in engineering*, 2014(1), 240565. <https://doi.org/10.1155/2014/240565>

[16] Ha, H., Zhang, B., & Lv, Z. (2003). A novel principle of single-ended fault location technique for EHV transmission lines. *IEEE transactions on power delivery*, 18(4), 1147–1151. <https://doi.org/10.1109/TPWRD.2003.817505>

[17] Joorabian, M., Asl, S. M. A. T., & Aggarwal, R. K. (2004). Accurate fault locator for EHV transmission lines based on radial basis function neural networks. *Electric power systems research*, 71(3), 195–202. <https://doi.org/10.1016/j.epsr.2004.02.002>

[18] Gayathri, K., & Kumarappan, N. (2010). Accurate fault location on EHV lines using both RBF based support vector machine and SCALCG based neural network. *Expert systems with applications*, 37(12), 8822–8830. <https://doi.org/10.1016/j.eswa.2010.06.016>

[19] Kimbark, E. W. (1976). Selective-pole switching of long double-circuit EHV line. *IEEE transactions on power apparatus and systems*, 95(1), 219–230. <https://doi.org/10.1109/T-PAS.1976.32095>

[20] Al-Rawi, A. M., & Slivinsky, C. (1990). Computation of secondary arc current on double-circuit EHV lines employing single-pole switching. *Electric power systems research*, 18(2), 131–140. [https://doi.org/10.1016/0378-7796\(90\)90016-V](https://doi.org/10.1016/0378-7796(90)90016-V)

[21] Hesse, M. H., & Sabath, J. (1971). EHV double-circuit untransposed transmission line-analysis and tests. *IEEE transactions on power apparatus and systems*, (3), 984–992. <https://doi.org/10.1109/TPAS.1971.292839>

[22] Rizk, F. A. M. (2016). Modeling of UHV and double-circuit EHV transmission-line exposure to direct lightning strikes. *IEEE transactions on power delivery*, 32(4), 1739–1747. <https://doi.org/10.1109/TPWRD.2016.2592801>

[23] Gayathri, K., & Kumarappan, N. (2015). Double circuit EHV transmission lines fault location with RBF based support vector machine and reconstructed input scaled conjugate gradient based neural network. *International journal of computational intelligence systems*, 8(1), 95–105. <https://doi.org/10.2991/ijcis.2015.8.1.8>

[24] Gurmu, E. D., Bole, B. K., & Koya, P. R. (2021). Optimal control strategy on the transmission dynamics of human papillomavirus (HPV) and human immunodeficiency viruses (HIV) coinfection. *International journal of research in industrial engineering*, 10(4), 318–331. <https://doi.org/10.22105/riej.2021.294463.1234>

[25] Tabatabaei, H., & Memari, M. (2019). Optimal control design for linear-invariant linear singular systems with time using orthogonal functions. *Journal of decisions and operations research*, 4(3), 262–275. (In Persian). <https://doi.org/10.22105/dmor.2019.184852.1119>

[26] Rabbi, M. F., Chakrabarty, N., & Shefa, J. (2018). Implementation of fuzzy rule-based algorithms in p control chart to improve the performance of statistical process control. *International journal of research in industrial engineering*, 7(4), 441–459. <https://doi.org/10.22105/riej.2018.150727.1062>

[27] Jahangiri, M., Farrokhi, A., & Amirabadi, A. (2021). Designing novel LDO voltage regulator implementation on FPGA using neural network. *Journal of applied research on industrial engineering*, 8(3), 205–212. <https://doi.org/10.22105/jarie.2021.270076.1244>

[28] Kumar, A. N., Chakravarthy, M., Kumar, M. S., Nagaraju, M., Ramesha, M., Gururaj, B., & Kiran, E. U. (2023). Fuzzy location algorithm for cross-country and evolving faults in EHV transmission line. *International journal of fuzzy logic and intelligent systems*, 23(2), 130–139. <https://doi.org/10.5391/IJFIS.2023.23.2.130>

[29] Yadav, A., & Swetapadma, A. (2015). Enhancing the performance of transmission line directional relaying, fault classification and fault location schemes using fuzzy inference system. *IET generation, transmission & distribution*, 9(6), 580–591. <https://doi.org/10.1049/iet-gtd.2014.0498>

[30] Naresh Kumar, A., Sanjay, C., & Chakravarthy, M. (2019). Fuzzy expert system based protection for double circuit incomplete journey transmission lines. *International journal of computational intelligence & IoT*, 2(1), 351–355. <https://ssrn.com/abstract=3355297>

[31] Srikanth, B., Kumar, A. N., & Sridhar, P. (2022). Four circuit transmission line location for inter circuit faults using fuzzy expert system. *Journal européen des systèmes automatisés*, 55(2), 273. <https://doi.org/10.18280/jesa.550216>

[32] Kumar, N., Sanjay, C., & Chakravarthy, M. (2020). Mamdani fuzzy expert system based directional relaying approach for six-phase transmission line. *International journal of interactive multimedia and artificial intelligence*, 6(1), 41–50. <https://doi.org/10.9781/ijimai.2019.06.002>

[33] Guillaume, S., & Charnomordic, B. (2010). Interpretable fuzzy inference systems for cooperation of expert knowledge and data in agricultural applications using fispro. *International conference on fuzzy systems* (pp. 1–8). IEEE. <https://doi.org/10.1109/FUZZY.2010.5584673>

[34] Guillaume, S., & Charnomordic, B. (2011). Learning interpretable fuzzy inference systems with FisPro. *Information sciences*, 181(20), 4409–4427. <https://doi.org/10.1016/j.ins.2011.03.025>

[35] Guillaume, S., & Charnomordic, B. (2012). Fuzzy inference systems: An integrated modeling environment for collaboration between expert knowledge and data using FisPro. *Expert systems with applications*, 39(10), 8744–8755. <https://doi.org/10.1016/j.eswa.2012.01.206>

[36] Kumar, A. N., Sanjay, C., & Chakravarthy, M. (2020). A single-end directional relaying scheme for double-circuit transmission line using fuzzy expert system. *Complex & intelligent systems*, 6, 335–346. <https://doi.org/10.1007/s40747-020-00131-w>

[37] Singh, A., Herunde, H., & Furtado, F. (2020). Modified Haar-cascade model for face detection issues. *International journal of research in industrial engineering*, 9(2), 143–171. <https://doi.org/10.22105/riej.2020.226857.1129>

[38] Mahalakshmi, P., Vimala, J., Jeevitha, K., & Nithya Sri, S. (2024). Advancing cybersecurity strategies for multinational corporations: novel distance measures in q-rung orthopair multi-fuzzy systems. *Journal of operational and strategic analytics*, 2(1), 49–55. <https://doi.org/10.56578/josa020105>

[39] Mandal, S., & Jayaram, B. (2015). SISO fuzzy relational inference systems based on fuzzy implications are universal approximators. *Fuzzy sets and systems*, 277, 1–21. <https://doi.org/10.1016/j.fss.2014.10.003>

[40] Shafi, L., Jain, S., Agarwal, P., Iqbal, P., & Sheergojri, A. R. (2024). An improved fuzzy time series forecasting model based on hesitant fuzzy sets. *Journal of fuzzy extension and applications*, 5(2), 173–189. <https://doi.org/10.22105/jfea.2024.432442.1357>

[41] Hatami, A., & Kazemipoor, H. (2013). Fuzzy big-M method for solving fuzzy linear programs with trapezoidal fuzzy numbers. *International journal of research in industrial engineering*, 2(3), 1–9. https://www.riejournal.com/article_47945.html

[42] Zadeh, L. A. (1965). Fuzzy sets. *Informatio and control*, 8(3), 338-353. [https://doi.org/10.1016/S0019-9958\(65\)90241-X](https://doi.org/10.1016/S0019-9958(65)90241-X)

[43] Pabarja, R., Jamali, G., Salimifard, K., & Ghorbanpur, A. (2024). Analysis of the LARG of the hospital medical equipment supply chain using the fuzzy inference system. *International journal of research in industrial engineering* (2783-1337), 13(2), 116–151. <https://doi.org/10.22105/riej.2024.431679.1408>

[44] Darwito, P. A., & Indayu, N. (2023). Adaptive neuro-fuzzy inference system based on sliding mode control for quadcopter trajectory tracking with the presence of external disturbance. *Journal of intelligent systems and control*, 2(1), 33–46. <https://doi.org/10.56578/jisc020104>